universität wien

BACHELOR THESIS

Title of the Bachelor thesis

Neutron Interferometry

Aspired academic degree

Bachelor of Science

Author:	Christian G. KNOBLOCH
Student ID Number:	0846069
Degree Courses:	Physics
assisted by:	Univ-Prof. Dr. Reinhold BERTLMANN
and by:	Univ-Prof. Dr. Markus ASPELMEYER

Vienna, on the 19th of September 2011

1 Abstract

On the following pages I describe a very young field in physics and especially in quantum physics: *neutron interferometry*. Although the realization of this measuring method was worked out rather recently, the important successes achieved through its many applications have soon caused it to constitute an own important field. The multitude of applications range from simple spin experiments to the determination of extradimensions in our own galaxy. It has been shown that moreover, for all these applications *neutron interferometry* is a very accurate measuring method. Having become an indispensable tool in nearly every field of quantum physics research, the study of *neutron interferometry* is an up-to-date issue. With special emphasis placed on its basic physical understanding I did not focus on the highly specialized experimental setups that can be performed by means of a neutron interferometer, that is, the present study aims at giving the reader an extensive overview of the many possible applications in modern physics offered by *neutron interferometry*.

Table of Contents

1 Introduction

In 1974, the research group of H. Rauch at the Vienna *Atominstitut*, Vienna Technical University, performed the first experiment on interfering neutrons, which gave us the fascinating confirmation, that the formula by de Broglie is also true for neutrons. They were able to show the dual wave and particle behavior for neutrons adapting an interferometer, which Bonse and Hart had originally constructed for the use with X-rays. Consecutively, many experiments on neutron interferometry have been set up for various purposes and neutron interferometry got developed very fast.

The present paper gives a general review of the neutron interferometry techniques, then points out the phase shift phenomena in neutron interferometry and closes with an overview of the related applications.

2 Neutrons—Classical Description and Quantum Approach

2.1 Facts about neutrons

Neutrons belong to the constituent particles of the atomic nucleus and possess a neutral electric charge. Similar to baryons, neutrons are made of quarks, that is of two down quarks and one up quark; they have a rest energy of about $939,57\text{MeV}$, which is equivalent to a rest mass of $\sim 1,67 \cdot 10^{-27} kg$. The mean lifetime of a free neutron is $T_{1/2} = 885,8(9)s$, that is nearly 15 minutes. Furthermore, the neutron is classified as a fermion that is as a particle with half-integer spin.

Neutrons, which are suitable for the use in our experiments usually arise from a source using nuclear fission of ^{235}U. When the fission is achieved the produced neutrons slow by elastic shocks in the hydrogen moderator and remain 'thermalized'. The following table lists the properties of thermal neutrons:

THERMAL NEUTRONS	VALUE
Temperature	293,6 K
Energy	0,0253 eV
Velocity	2200,05 m/s
Wavelength	0,17982 nm

From the reactor source the thermal neutrons get directed via a neutron guide to the experimental setup being currently run. The phase space density of the strongest known neutron sources is referred to be 10^{-14}, which corresponds to the occupation number in the coherence volume. For that reason we can assume that the probability of having two interacting neutrons in our coherence

volume can be set to zero. This is an important point, because we can assume now, that all the detected neutrons are free from any correlation.

2.2 Quantum description of neutrons, 4π spinor systems

As indicated in the previous section, neutrons are fermions, thereby possessing spin-$\frac{1}{2}$. To submit a neutron to rotation we apply the corresponding quantum formalism and denote the rotated state of such a spin-$\frac{1}{2}$ system by

$$|\psi\rangle_r = D_z(\phi)|\psi\rangle, \tag{2.1}$$

where the index r means the rotated spin state and $D_z(\phi)$ is the rotation operator for such a system, written by

$$D_z(\phi) = \exp\left(\frac{-\mathrm{i}\mathcal{S}_\mathrm{z}}{\hbar}\right). \tag{2.2}$$

Applying the above onto our state, which we write as $\binom{\psi_1}{\psi_2}$ for an easier understanding, and inserting the spin matrix for spin-$\frac{1}{2}$particles, that is

$$S_z = \frac{\hbar}{2}\begin{pmatrix}1 & 0\\ 0 & -1\end{pmatrix}, \tag{2.3}$$

we obtain

$$\exp\left(-\frac{\mathrm{i}\mathcal{S}_\mathrm{z}}{\hbar}\right)|\psi\rangle = \begin{pmatrix}e^{-\frac{\mathrm{i}}{2}} & 0\\ 0 & e^{\frac{\mathrm{i}}{2}}\end{pmatrix}\begin{pmatrix}\psi_1\\ \psi_2\end{pmatrix} = \begin{pmatrix}e^{-\frac{\mathrm{i}}{2}}\psi_1\\ e^{\frac{\mathrm{i}}{2}}\psi_2\end{pmatrix}. \tag{2.4}$$

Choosing an angle of 2π for ϕ, we can calculate that the outcoming result is no longer the original vector but has become $-|\psi\rangle$.

It is then easily checked that if we rotate the neutron by 4π it will turn back into its initial state. For this reason neutrons are called 4π spinor systems in quantum mechanics.

2.3 Detecting neutrons

In general terms, neutron detectors divide into two different categories, which are appropriate to identify the presence of namely either the fast or the slow neutrons. In the present study I will limit to a close consideration of the slow neutron detector type, because this is the one which we need when performing experiments that involve neutrons. This type of detector mainly consists of two separate parts, the first one being a tube filled with a special gas and the second part being a material that gives rise to the scintillation process. It must be pointed out that apart from gas detectors there exists another detector type, which uses appropriate solid matter instead of gas to trace the existence of neutrons, but most of the experiments cited in the following did apply gas detectors. Since it is not, or almost not, possible to directly detect

neutrons—the neutral charge of which do not class them as typical ionizing particles—the working principle of such gas detector takes profit of particles with a high neutron cross section added to its filling. An example to illustrate such skilful detour is the He^3 detector. Thermal neutrons enter the volume filled with the He^3 gas and get absorbed by it. The products of this reaction are ${}_1H^1$ and ${}_1H^3$ ions which the scintillator is able to respond to.

3 Interferometry in Quantum Physics

Looking back to the historical development of modern physics it can be said that quantum physics started with the postulation by a number of physicists, which then was strongly held up by Albert Einstein, that there is no two ways about it that photons are manifested in the dual nature of a wave and a particle as well. The big step de Broglie took forward in 1924 was, that he inverted this postulate and gave us a formula which enables us to calculate the wavelength of every particle we could imagine.

$$\lambda = \frac{h}{p} = \frac{h}{mv}\sqrt{1 - \frac{v^2}{c^2}}. \tag{3.1}$$

Since we have adopted this fundamental concept, interferometry in quantum physics has kept growing in importance, turning even into the essential tool to testify the quantum behaviour of a system. From that development onwards, so many a different type of interferometer has come to be applied with quantum mechanical experiments that I will give a closer review on them before introducing the neutron interferometer itself.

To put it simply, an interferometer uses the property of waves to split a wavefront into two, or more, mostly equal parts. The two coherent parts getting stably recombined after a while thereby give us an interference pattern that allows us to make statements about the properties of the object under investigation, that is, about the wavefunction describing the object.

Several types of different interferometers have been designed to this day, among these some are still well known whereas others remain nearly unknown. The 'Michelson interferometer' for instance played the essential part in the experiment that knocked out the theory of light aether. Another famous one, which came to frequent use in quantum mechanics, is the 'Mach-Zehnder interferometer'.

This type of interferometer is well known for various experiments, an example is the 'bomb experiment'. The optics setting makes that the incoming wave is split by a beamsplitter that reflects 50% of the beam and transmits the other 50%. After having passed the beamsplitter the two beams get reflected at a mirror, and one of the beams, or both together pass a phase shifter, which could be made of a material to be investigated, for instance. The last step is

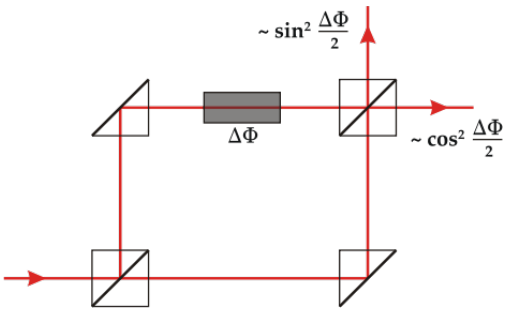

Figure 3.1 Schematic representation of a Mach-Zehnder interferometer with a phase shifter in its upper beam path | ©Wikipedia

the second beamsplitter giving the two beams the chance to interfere again and to cause a click count in one of the possible detectors mounted thereafter.

4 Neutron Interferometry

The basic design of the different neutron interferometry setups remains basically the same and looks very similar to the 'Mach-Zehnder interferometer'. We consider an incoming beam, we have it split and then let it interfere again at a certain point. The first scientist who thought about realizing an interferometer that works for neutrons had been *Helmut Rauch* in 1974. Rauch adapted the so-called 'three-crystal interferometer' by Bonse and Hart, who had conceived it for X-rays nearly a decade earlier, and thus could perform an experiment with unpolarized monochromatic neutrons. The 'three-crystal interferometer', and all the later developments of neutron interferometers alike, are made from a single monolithic silicon crystal. Out of it the interferometer gets cut in one piece. The name 'three-crystal interferometer' might appear confusing, however the denomination refers to the three parallel plates (usually in 220 crystal orientation) of a perfect crystal structure which the neutron beam passes all through. An illustration and a photograph picture of such a neutron interferometer are shown below.

4.1 Operating principle, Bragg reflection

Why do we need a monolithic silicon crystal? The big idea by Rauch, or by Bose and Hardt respectively, consisted in introducing the process of Bragg diffraction into interferometry. Bragg's law describes how a particle with wavelength λ gets scattered at several layers of an anisotropic material, what our silicon crystal actually is,

$$2d \cdot \sin\Theta = n\lambda, \tag{4.1}$$

where d is the distance that separates the neighbour crystal planes, and where Θ denotes the Bragg angle, which however is not equivalent to the diffraction

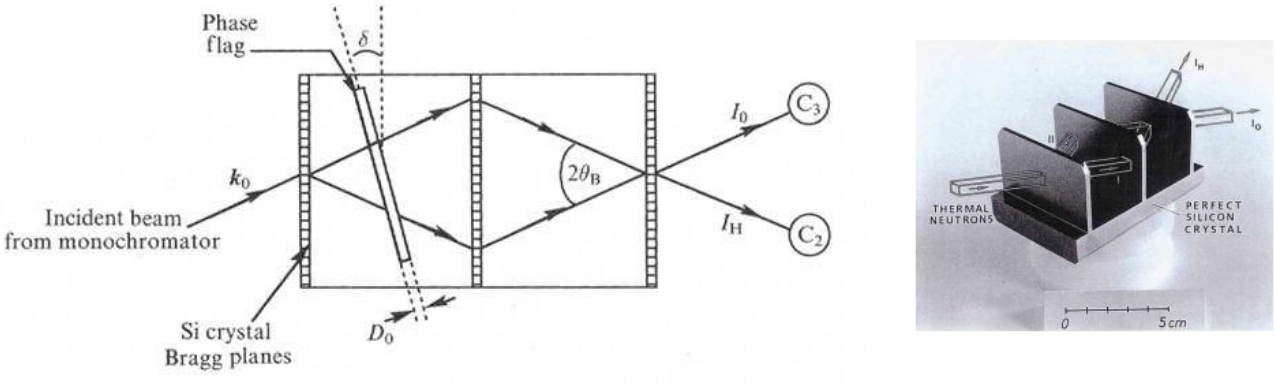

Figure 4.1 Schematic representation and picture of the first monolithic 'three-crystal interferometer'. | ©David Kendellen:"Neutron Interferometry and 4π Spinor Symmetry Experiments"(l); www.teilchen.at(r)

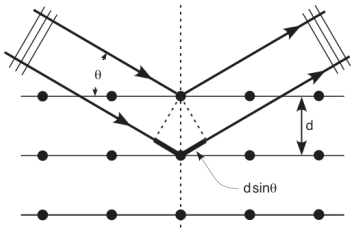

Figure 4.2 Derivation of Bragg's law: The incoming wavefront enters from the left and gets scattered at the atoms of the crystalline planes. ©Free Software Foundation

angle—as we have come to understand at the basic courses in optics—but which is rather the angle between the planes and the incoming beam. The illustration below should make this equation more clear.

As we mentioned before, the wavelengths of the thermal neutrons used in the real experiments range about $1 - 4$Å. If we want to obtain a diffraction angle 2Θ of about 45° we rather have to use neutrons of the upper range values of wavelength. Applying all these criteria onto Bragg's diffraction law we will recognize that we have to look for a material the spacing between the crystal planes of which ranges about 3Å. A first class material and probably the one with the best fitting parameters, and moreover, of a high quality produced on industrial-scale, which altogether satisfies this condition is *silicon*.

We can see in figure 4.1 that the neutron beam passes the crystal blades of each about $4,3954 \pm 0,0008$ *mm* thickness at three times. In literature we can often read that the first and the last blade work both as beamsplitters whereas the central one corresponds to a mirror, however, this appears so when we consider the arrangement broadly. Under a closer inspection we will recognize that the central plate does work in the very same way as the other two and that

the edge beams leave the interferometer. With such a type of interferometer the two particle paths can be separated by about 5 *cm*.

4.2 Phase shifts and intensities

To testify the quantum behaviour of a system we have to measure its wave behaviour, plus, to evaluate the various effects that result from my changing the different parameters of my interferometer. In common interferometers such a change is for instance obtained by varying the length of one arm of the interferometer. In neutron interferometry we hardly can vary the length because of our solid monolithic silicon crystal, so what is done in the most experiments is getting a slab of a different material inserted into the beam paths. The effects caused by such procedure are discussed in the present chapter.

First I will consider the phase of the wavefunction, which the source emits and which is denoted by $\Phi(x,t)$, as a scalar field. This phase evolves in time, while the two beams continue their path through the interferometer and can be described by a line integral over the Lagrangian

$$\Phi(x,t) = \frac{1}{\hbar}\int \mathcal{L}\cdot \mathrm{dt}', \tag{4.2}$$

where the Lagrangian can be written in terms of the Hamiltonian $\mathcal{H}$, the momentum of the particle p and its classical group velocity v, namely $\mathcal{L} = \mathrm{p}\cdot\mathrm{v} - \mathcal{H}$.

Inserting this into (4.2) we get the final phase the neutron wave posesses at its hitting the detector, that is

$$\Phi(x,t) = \frac{1}{\hbar}\left[\int_{x_0}^{x} p\cdot ds - \int_{t_0}^{t}\mathcal{H}\cdot \mathrm{dt}'\right] = \int_{x_0}^{x} k\cdot ds - \int_{t_0}^{t}\omega\cdot dt', \tag{4.3}$$

with the wave vector k and the frequency ω. To distinguish the possible traveling paths of the neutrons across the interferometer we assign (4.3) index 1 to the upper and index 2 to the lower path, respectively. Doing this, one can define the phase difference achieved at the detector by

$$\Delta\Phi(x,t) = \Phi_2(x,t) - \Phi_1(x,t). \tag{4.4}$$

As we can easily imagine, getting an invariant phase difference in our interferometer will not reveal anything of interesting to us. Therefore, we have to include an extra phase shift into one of the two paths and cast an eye on what happens to the resulting interference of the beams. For that purpose we introduce a potential-induced phase shift with respect to the original phase difference that is defined by

$$\Delta\Phi_V = \Delta\Phi - \Delta\Phi_0, \tag{4.5}$$

whereat we read the phase difference of the beams at zero potential as $\Delta\Phi_0$. Using the notation of (4.3), we can write

$$\Delta\Phi_V(x,t) = \frac{1}{\hbar}\left[\int_{x_0}^{x}\Delta p_2\cdot ds - \int_{x_0}^{x}\Delta p_1\cdot ds - \int_{t_0}^{t}\Delta\mathcal{H}_2\cdot \mathrm{dt}' + \int_{\mathrm{t_0}}^{\mathrm{t}}\Delta\mathcal{H}_1\cdot \mathrm{dt}'\right]. \tag{4.6}$$

There are different possible ways to cause a potential-induced phase shift, three of which we will take a closer look at in the following.

1. The most common method to implement a potential is to insert something, for instance a material, into one path of the interferometer. This causes a potential, which changes my phase depending on the position of the entered material, but which remains time-invariant, that is $V = V(x)$. Traveling across the potential distance, the neutron is decelerated at the one end and accelerated at the other end. The time-invariance of this setup yields that the Hamiltonian drops out of the equation. So, only the change of the kinetic momentum remains to evaluate the equation, we get

$$\Delta\Phi_V(x) = \frac{1}{\hbar}\int_R \Delta p_{kin} ds, \tag{4.7}$$

   for this experimental setup, where the index R stands for the area of the potential involved.

2. Another configuration is obtained by applying a potential which depends upon time only, that is, a pulsed potential that remains invariant along x. So the time-dependent Hamiltonian is the only remaining term of the equation. we get

$$\Delta\Phi_V(t) = -\frac{1}{\hbar}\int_{pulse}\Delta\mathcal{H}(\mathrm{t}')\mathrm{dt}'. \tag{4.8}$$

3. A third interesting configuration takes care that the phase shift depends on the geometry and the topology of the setting up only. In this case, a hidden momentum arises, the effect of which I will not discuss in detail here [5].

Now our focus should lay upon the neutron beam intensities that are signalized by the detectors, because these intensity measurements give evidence of the experimentally gained information we are aiming at. For such purpose we use the notation of Werner and Rauch as displayed in the figure 4.1. Therein, the authors define the wave functions as depending of the phases of the paths X, the original entering wave function is denoted by ψ_0 and the coefficients of transmission and reflection are denoted by 't' and 'r', respectively. The denoting is completed by defining the resulting beams that leave the interferometer after the third crystal plate as the O-beam and the H-beam, respectively. Applying this notation, the intensity of the O-beam satisfies the equation

$$I_O = |\psi_1 + \psi_2|^2 = |trr\psi_0 e^{i\mathrm{X}_1} + rrt\psi_0 e^{i\mathrm{X}_2}|^2, \tag{4.9}$$

where the indices 1 and 2 mark the different paths in the interferometer the neutrons travel along. One now can easily effectuate the multiplication and explicitly write down the result by

$$I_O(\Delta \mathrm{X}) = A\,(1 + \cos \Delta \mathrm{X})\,. \tag{4.10}$$

ΔX is the phase difference achieved between the two different paths X_1 and X_2 and the constant A takes mainly account of the transmittivity and the reflectivity coefficients and is defined by $A = |\psi_0|^2 \cdot \left(|r|^4|t|^2\right)$. Similarly, the H-beam is described by the equation

$$I_H(\Delta \mathrm{X}) = |trt\psi_0 e^{i\mathrm{X}_1} + rrr\psi_0 e^{i\mathrm{X}_2}|^2 = B - A\cos \Delta \mathrm{X}, \tag{4.11}$$

where the constant B stands for $B = |\psi_0|^2 \cdot \left(|t|^4|r|^2 + |r|^6\right)$. If we consider that zero neutrons get absorbed by the silicon slabs we can say, that $I_O + I_H =$ constant. So we see that the resulting intensities exhibit the behaviour of a cosine wave oscillator. This theoretically predicted behaviour could also experimentally be confirmed. An example of such an interference pattern is shown below.

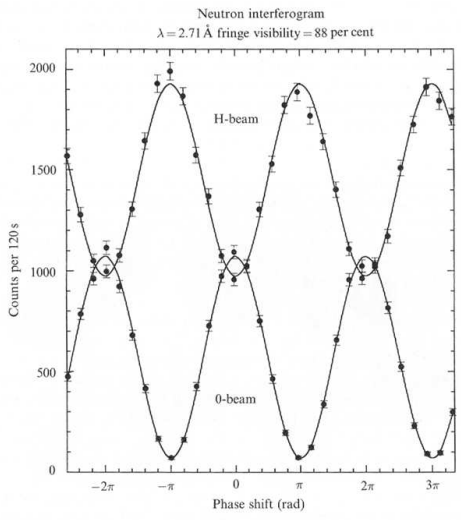

Figure 4.3 Interference pattern for the O-beam and the H-beam, respectively: One easily distinguishes a cosine wave oscillation.|©M.Arif and D.L.Jacobson, NIST, 1997

4.3 Phase shift caused by neutron-nuclei interaction

When the neutrons pass the flag of the inserted phase shifting material, they undergo a so-called optical potential, which we want to examine in detail in this chapter. Such potential can generally be expressed by

$$V_{opt} = \frac{2\pi\hbar^2 bN}{m}, \tag{4.12}$$

where N is the atom density and b stands for the nuclear scattering amplitude of the neutrons. To be able to insert this potential into our equations of the previous section we have to establish a link to the momentum of the neutron particle, which we found to be the only term that is left in equation (4.7). For

this purpose we strain the fact that the energy $Epsilon_0$ is retained unchanged in this situation. This yields

$$\mathrm{E}_0 = \frac{p_0^2}{2m} = \frac{p^2}{2m} + V_{opt}. \tag{4.13}$$

From above we can deduce the resulting phase shift as

$$\Delta p = p - p_0 \approx -\frac{1}{2}\frac{V_{opt}}{\mathrm{E}_0} p_0. \tag{4.14}$$

This result we put into (4.7) and get

$$\Delta\Phi_{nuc} = \frac{1}{\hbar}\int_0^L \Delta p \cdot ds = -\frac{V_{opt}}{2\hbar \mathrm{E}_0} p_0 L = -\lambda_0 N\, b L \tag{4.15}$$

where L is the length of the optical potential, and $\lambda_0 = \frac{h}{p_0}$. Setting a typical optical potential of about $10^{-7}eV$ and, for instance, a 1mm thick aluminium slab the neutrons phase gets shifted by an angle of 420rad $\approx$ 1500000deg. This estimated example shows one big advantage of such type of neutron diffraction experimental setup, namely that neutron interferometry is a very sensitive measuring method.

4.4 Types of neutron interferometers

A better approach to a practicable classifying of the various types of neutron interferometers is given when we explain about the number of closed paths or loops in such interferometer: both single loop and double loop neutron interferometers could already be realized.

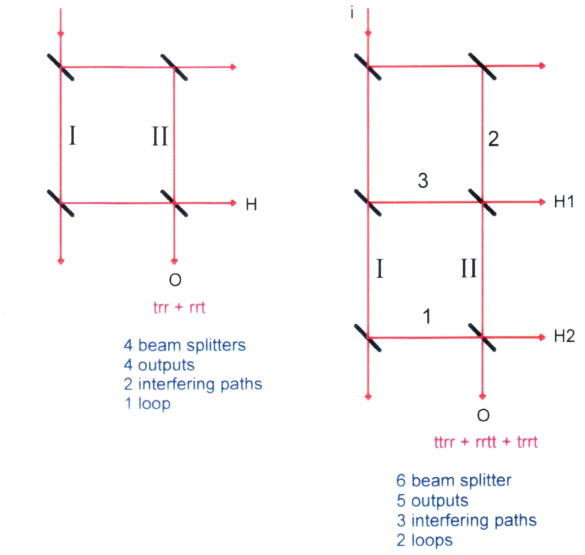

Figure 4.4 The basic settings for single-loop (left) and double-loop (right) interferometers | ©Michael Zawisky, Austrian Atomic Institute

From the above illustration it is understandable that the one-loop neutron interferometers have been known and realized since considerably earlier a time than the two-loop type are. For instance, the very first one-loop setting up was a three-crystal (LLL) interferometer. The reason for the difficulties met with the two-loop configuration can mainly been found with the technical limitations at producing a monolithic silicon crystal that were sufficiently large. Nowadays the biggest known interferometer of the type is of the length of 21cm, which is also the lenght of each path. The achieved optical separation of both pahts is about 5cm (state-of-the-art realization in 2005). Today, the principal limiting factor for the feasibility of still more efficient instruments lies at the limited technology of manufacturing still bigger crystals. Of course, the trend continues asking for extra-large-scale systems, which would provide experiments at a still higher accuracy.

A type of interferometer I also want to mention here is the so-called 'null-interferometer' by S.A. Werner.

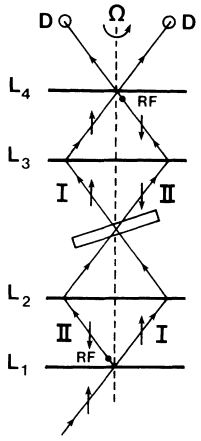

Figure 4.5 Proposal for the 'null-interferometer' | ©S.A. Werner

As one can easily see in figure 4.5, this type of interferometer is independent of influences like variations of the gravitational potential. Werner originally proposed this configuration to test the influence of the neutron spin-rotation coupling with the neutron phase.

Other real interferometers, that have been realized so far can be seen in figure 4.6.

5 Applications of Neutron Interferometry

5.1 4π spinor experiments

One of the first experiments, which was thought of, had been the observation of the 4π spinor symmetry in spin-$\frac{1}{2}$ systems, as I earlier explained in chapter (2). This experimental setup can easily be accomplished: Starting from a neutron

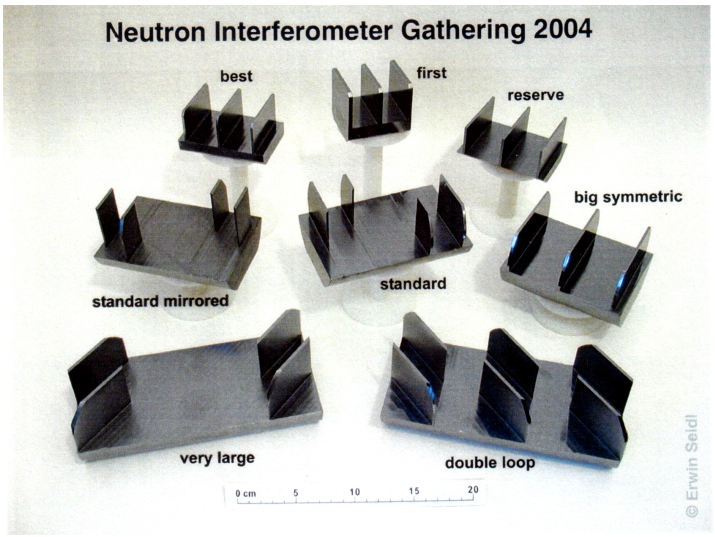

Figure 4.6 Several types of neutron interferometers produced at the Austrian Atomic Institute. | ©Erwin Seidl

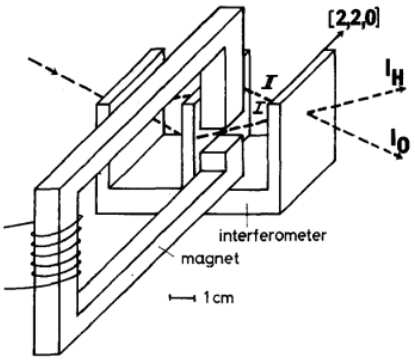

Figure 5.1 Experimental setup of the 4π spinor experiment run by Rauch et al. in 1975 | ©Ref.1

interferometer we just have to apply a magnetic field to the interferometer, as is seen by the following illustration (the Miller indices [2,2,0] standing for the chosen orientation of the silicon crystal).

As the neutron passes the magnetic field it couples as a dipole to the B-field. Therefore we are able to write the Hamiltonian in terms of the Pauli spin matrices σ as: $H = -\mu \cdot B = -\mu\sigma \cdot B$. The neutron then crosses the magnetic field and for that reason gets affected by the Larmor precession and by the spinor rotation. This causes that the wavefunction no longer depends on time, it is only determined by the angle of rotation. This angle can be denoted as

$$\alpha \approx \frac{2\mu}{\hbar \mathrm{v}} \int B \cdot ds, \tag{5.1}$$

that is, as an integral along the neutrons trajectory, where v denotes its velocity. The intensity of the forward beam, the O beam, then satisfies the equation

$$I_O = |\psi_0(0) + \psi_0(\alpha)|^2 = 2|\tilde{\psi}_0|^2 \left(1 + \cos\left(\frac{\alpha}{2}\right)\right). \tag{5.2}$$

From the term that contains $\cos\left(\frac{\alpha}{2}\right)$ we can clearly see that the neutron gets back into its initial state by an angular rotation that is equivalent to 4π only. This has also been the result Rauch et al. recognized from their experimental intensity patterns, which we find reproduced in figure 5.2.

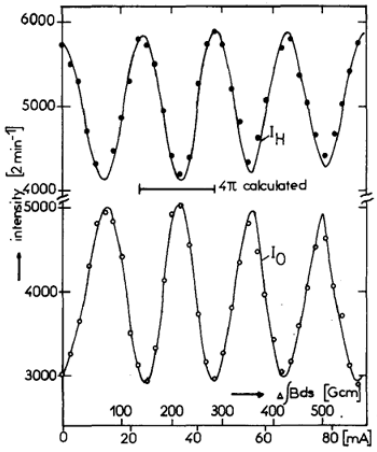

Figure 5.2 Intensity modulation resulting from the magnetic field influence at the two different optical paths of the interferometer | ©Rauch et al. 1975

5.2 Gravitation in neutron interferometry

In June 1975, the three authors R. Colella, A.W. Overhauser and S.A. Werner published an article in the *Physical Review Letters*, where they presented an experimental setup, which gets lovingly called COW experiment since then [6]. They considered an experimental setup, which would not limit the evaluation to a consideration of the Planck constant alone, but their configuration, moreover, should also make the gravitational constant assume its determining part. Until then, all experiments in neutron interferometry had been carried out at one same gravitational potential for each of the 'legs' of the interferometer. The 'COW' experiment would take profit of the fact that the neutrons, the mass of which is non-negligible when compared to that of photons, make the neutron interferometer become a perfect instrument to observe the influence that gravitation exerts on the wave function of particles. To explain this gravitational effect, I will largely follow their paper starting with the 'COW' experimental setup, which we can see in the picture below.

The main part therein constitutes the so-called (triple Laue) LLL three-crystal interferometer consisting again of a monolithic silicon crystal with three plane-parallel cut slabs of a thickness a, situated each at a distance of d from its neighbour slab. Next to this three-crystal there are mounted three single ^3He gas detectors (C1-C3), which the neutron beams will hit after their passing the

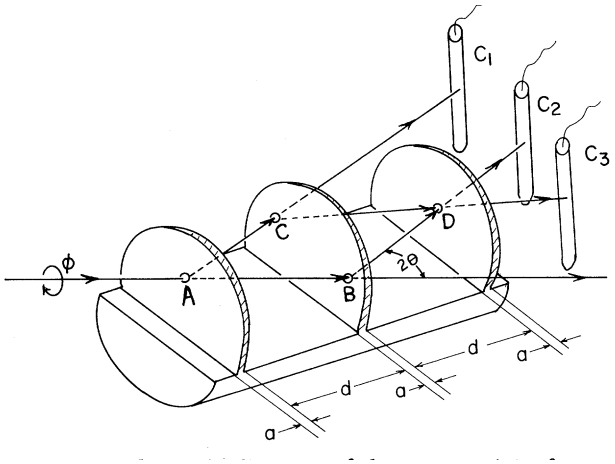

Figure 5.3 Schematic picture of the COW experimental setup. | ©Ref. 6

LLL three-crystal on the different paths, and the counting rates of which are used to obtain the intensity patterns for each of the neutron paths.

The basic idea of the 'COW' experiment now is to tilt the whole arrangement by an angle α to obtain a higher running path for the neutron wave and another one that is running at a lower height. In their first experiment the magnetic field induced rotation was performed along the AB axis of the incident beam. In principle, it is irrelevant along which axis of the setup the tilting is effected, the significance lays in obtaining an upper and a lower path to get a related difference in the gravitational potential. Note, that such rotating along AB will apply the same magnetic effect onto the neutrons when passing A or B and thus will give us the same quantum mechanical phase shift for the two different ways given by the segments AC and BD.

Assuming this potential to be a Newtonian one, we can describe it as a function of the rotation angle α by the equivalence

$$\Delta V\,(\alpha) = mgH_0 \sin(\alpha), \tag{5.3}$$

with m being the neutron mass, g the local gravitational acceleration and H_0 the perpendicular distance between the paths AB and CD. Using the constant of motion $\mathrm{E}_0 = \frac{\hbar^2 k_0^2}{2m}$, we can define a difference of the momenta of the two possible paths by

$$\Delta p = p - p_0 = -\frac{mgH_0 \sin(\alpha)}{2\mathrm{E}_0}. \tag{5.4}$$

This result we can apply to (4.7) to express a phase shift, thus yielding

$$\Delta\Phi_{grav} = \frac{1}{h}\oint \Delta p \cdot ds = -2\pi m^2 \frac{g}{h^2}\lambda_0 A_0 \sin(\alpha) \equiv q_{COW}\,\sin(\alpha), \tag{5.5}$$

where A_0 is the area enclosed by the two beam paths, given by $A_0 = (2d^2 + 2ad)\tan\Theta$, including the Bragg angle Θ for the silicon (220) reflections.The relative gravitational phase shift $\Delta\Phi_{grav}$ is defined as the specific phase shift

q_{COW} from the 'COW' experiment modulated by the sine wave of the tilting angle α.

In the first experiments run by the 'COW' group the setup was arranged in a way that the possible maximal tilting angles did not overcome $\pm 30 \neg \infty$. They calculated the difference between the intensities at the detectors C2 and C3, for which we have got the formulas in (4.10) and (4.11), and then plotted it versus the angle of tilting. The result can be seen from the graph shown below.

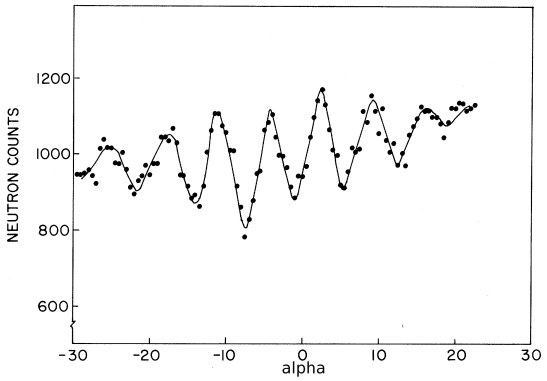

Figure 5.4 Counting rates representing $I_2 - I_3$ as a function of the rotating angle along the AB axis. | ©Ref. 6

Now this is not the whole game of it, because, as M.A. Horne has commented to the point, this type of experiments might not just be regarded as two path devices, but provide rather eight path interferometer setups instead [5]. For this reason, we have to replace our gravity phase shift formula (5.5) by a dynamical formula that takes account of the differing of the areas when swept by our wave function, or at least, we have to insert a correction term. This correction gives us a relation between q_{COW} and q_{grav}, the value for the gravitational phase shift becoming thereby relabeled from q_{COW} to q_{grav}.

$$q_{grav} = \left(1 + \frac{2a}{3d}\right) \cdot q_{COW} \,. \tag{5.6}$$

Moreover, interpreting that the non homogeneous aspect of the result displayed in figure 5.4 arises from an added up phase shift q_{grav} plus $q_{bending}$, which means that we also have to take account of the bending of the interferometer over its own weight, we will obtain, after Fourier transforming the datas, the result

$$q_{grav} + q_{bend} = 54,3 \text{ rad}, \tag{5.7}$$

which however was predicted from theory to be $q_{grav} = 59,6$ rad instead. Why did they have such a discrepancy? The authors of the 'COW'-experiments ascribed all this to the complexity around q_{bend}, what later on was understood not to be the case.

The case appeared to be more difficult than straight, when a group around Sam A. Werner found out that with their interferometer setup, the same

apparatus of which was designed to accept X-rays as well as neutrons passing through it, the value of this q_{bend} was determined to be $q_{bend} = 1,41$ rad. They could rely on a more accurate method of evaluation by inserting a phase rotator into one path of the interferometer and by scanning through its differernt angles δ at $\alpha_0 = 0$. They repeated the procedure for various angles α and thereby obtained an interferogram for each tilting angle. The difference between the resulting interferograms then is denoted by $\Delta\Phi_{grav}(\alpha)$. They also included a correction for the Sagnac effect with their interferometer setup (this effect taking account in a rotating interferometer of the parts of the neutron beams that are counter-propagating) and eventually got for the gravitational phase shift q_{grav} the following formula

$$q_{grav} = (q_{exp}^2 - q_{Sag}^2)^{\frac{1}{2}} - q_{bend}. \tag{5.8}$$

Taking all this into account they achieved a far better experimental evaluation, namely

$$q_{grav}(observed) = 58,72 \pm 0,03\text{rad}, \tag{5.9}$$

when compared with the theoretical calculation, that is $q_{grav}(theory) = 59,19\text{rad}$.

5.3 Verification of Berry's phase

5.3.1 Berry phase in general

Usually, when we speak about time evolution of a system, we use the Hamiltonian to calculate it, and, assuming that we have an adiabatic process, there will be no change in the functional form of the system. However, for a given state $|\psi\rangle$ this is only true up to a phase, where $|\psi(\tau)\rangle = e^{i\phi}|\psi(0)\rangle$. So we can say, that the state has got a memory of the way the wavefunction evolves, even if it goes back to its initial state. This extra phase depends on the surface, which is enclosed by this state evolution. It is not the only phase a given state might pick up during its evolution. There is a dynamical phase as well that is acquired over the course of a cycle, and so we can write the looping back of the whole state into its initial state as

$$|\psi(\tau)\rangle = e^{i\phi_D} e^{i\phi_G} |\psi(0)\rangle, \tag{5.10}$$

where $\phi_D = \phi_D(\tau)$ denotes the dynamical phase and ϕ_G, the geometrical phase, also known as the Berry phase. At this point it is neccessary to point out that such geometrical phase is manifest in a quantum mechanical system only, because classically we would consider the intensities marked by a detector and which are given by the integral of the square value of the wavefunction over a defined space area. So both the Berry phase and the memorizing of the track being travelled along constitute a purely quantum mechanical phenomenon.

For instance, a neutron with a spin angular momentum of $S = \frac{1}{2}\hbar$, which passes a magnetic field, is coupled by its spin to the B vector and interact with it performing a Larmor precession. If the externally applied magnetic field now rotates by an angle of α the wavefunction of the neutron particle will acquire a geometrical phase of $\phi_G = -\frac{1}{2}\alpha$, this change in phase being continuous.

- *CLASSICAL PARALLEL TRANSPORT*

The Berry phase can be easily understood if, first, we study the classical parallel transport, which describes the basic concept in a simple way. For this purpose we consider the figure below.

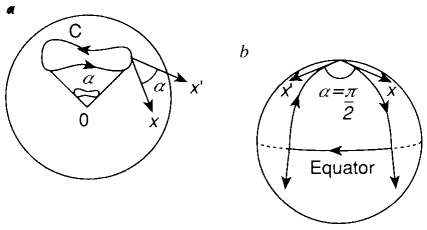

Figure 5.5 Classical parallel transport of a vector along a spherical surface: (a) For a closed curve in general, and (b) For a special curve | ©Ref. 7

Let us assume having a spherical surface as it can be seen for instance in figure 5.5. Having a vector that is, for instance, tangential to this surface, parallel transport occurs when the vector does not change its length and when it remains a tangent vector at each surface point of the sphere. The curve does not necessarily have to follow a spherical surface, its course may rather take place along any conceivable n-dimensional surface, on the limiting condition however, that such surface does exhibit a curvature. One can easily understand that there would not be involved any angle at all if the parallel transport occurred along a flat plane.

The angle, which appears in the geometric phase, is equal to the angle at the sphere's centre and which is related to the closed curve at the sphere's surface. When considering for instance a sphere such angle is $\alpha = \frac{A}{r^2}$, where A denotes the surface area surrounded by the closed curve and where $\frac{1}{r^2}$ corresponds to the curvature at each surface point.

Applying this same concept onto our general illustration of figure 5.5, we consider the vector that originates at the north pole and let it undergo a parallel transport down to the equator, along which we continue for a quarter of the whole possible extent. Then, from the equator, we let the vector undergo a reverse parallel transport back to the north pole and, as one can easily see, thereby the start and stop position of the vector are deviated by an angle $\alpha = \frac{\pi}{2}$.

In literature one often finds that the analogy to the classical Foucault-pendulum is referred to, what basically corresponds to the same reflection.

In general, all suitable possibilities to transport a vector along a surface can be defined by rules, called 'connections' on this area.

- QUANTUM BERRY PHASE

When considering all states that differ in phase only, the related class designates a ray in a vector space. Then, through combining all normalized states contained in such ray over the vector space we obtain the bundle of rays, which exhibit a natural connection. Thereby the phases of neighbouring rays can be compared to each other. Applying the conditions that eliminate the dynamical phase factor then yields a rule for the geometric phase of the system upon parallel transport.

Another point of view [7] denotes the set of rays in a Hilbert space $\mathcal{H}$ as a projective Hilbert space $\mathcal{P}$. To formulate a rule for the case of parallel transport the examination is concentrated onto a set of spin vectors. For that purpose, a curve p deploying on the surface of the sphere of $\mathcal{P}$ is defined in a way that $p(s)$ describes each point along this same curve. Now we consider a vector $|\psi(s)\rangle$ from the ray with $p(s)$ describing its smooth variations along the course of the curve. Assuming now that the length of $|\psi(s)\rangle$ remains observed during the parallel transport and that both $|\psi(s)\rangle$ and $|\psi(s+ds)\rangle$ retain the same phase, we have made ready the conditions which allow us to apply the following equation

$$\langle\psi(s)|\frac{d}{ds}|\psi(s)\rangle = 0. \tag{5.11}$$

Above relation constitutes the connection which gives us the rule for parallel transport of $|\psi(s)\rangle$ along any curve $p(s)$ in the projective Hilbert-space $\mathcal{P}$ under consideration.

In general, we can now calculate the phases of a given quantum mechanical system, having learnt that the whole phase Ω after the cyclic evolution of the state is given by a dynamical as well as a geometrical phase, namely $\Phi = \phi_D + \phi_G$. The dynamical phase can be written as

$$\phi_D = -\frac{1}{\hbar}\int_0^\tau \langle\psi(t)|H(t)|\psi(t)\rangle dt, \tag{5.12}$$

employing the Hamiltonian $H(t)$, whereas the geometrical phase can be formulated as

$$\phi_G = i\int_0^\tau \langle\psi(t)|\frac{d}{dt}|\psi(t)\rangle dt = i\oint_C \langle\psi(t)|D|\psi(t)\rangle ds, \tag{5.13}$$

employing the differential operator D on $\mathcal{P}$. Taking up again the spin-$\frac{1}{2}$ case of the neutron one will be able to write the above equations in a simpler form, that is,

$$\phi_D = -\frac{1}{2}\int_0^\tau \omega_L(t)\cos\gamma(t)dt \quad \text{and} \quad \Phi_G = -\frac{1}{2}\alpha, \tag{5.14}$$

with $\omega_L(t)$ describing the Larmor-precession and α being the angle that arises due to the parallel transport.

Soon after its rediscovery in 1984, the geometric phase got verified and was first observed in an experiment about an optical fiber [12]: The research group of A. Tomita et al. intentionally wounded the optical fiber to show that the passing light would pick up an additional phase, and, which would depend on the geometrical setup only.

5.3.2 Neutron experiments on Berry's phase

To carry on the investigations about the Berry phase using neutron interferometry considerably longer a time would pass by. In April 1996, the research group of Y. Hasegawa, M. Zawisky and H. Rauch published a paper, wherein they presented the observations made about the Berry phase in their neutron experimental setup.

In the course of their experiment they had made the assumption we met in the previous subsection, that is, the whole phase of the system is composed by a dynamical and a geometrical phase, $\Phi = \phi_D + \phi_G$. To measure just the geometrical phase it is therefore necessary to find a setup the configuration of which gets the dynamical phase to vanish. As we noted earlier, the dynamical phase is given by (5.12), which we will write, relating to the Hilbert space $\mathcal{H}$, in terms of the shift of the angular frequency $\Delta\omega$ to become

$$\Phi_D = \int_0^\tau \langle\psi(t)| - \Delta\omega dt|\psi(t)\rangle = \int_0^\tau -\Delta\omega dt. \tag{5.15}$$

To apply this formula to a neutron split-beam experiment we refer to the usual way of describing the phase in a wavefunction as being given by $k \cdot l - \omega t$.

Making use of this notation leads us to rewriting the dynamical phase for the change of the wavevector Δk in each path of the interferometer (paths 1 and 2, respectively) as

$$\phi_D = \frac{\int_{l_1}\langle\psi_1|\psi_1\rangle\Delta k_1 \cdot dl}{\langle\psi|\psi\rangle} + \frac{\int_{l_2}\langle\psi_2|\psi_2\rangle\Delta k_2 \cdot dl}{\langle\psi|\psi\rangle}. \tag{5.16}$$

To better explain the measuring results the above might preferably be expressed in terms of intensities I at the detectors, or, rather in terms of the transmission probability T of the absorber inserted into the beam path 2, such terms remaining each combined with the corresponding phase shift X. Thus we obtain

$$\phi_D = \frac{I_1}{(I_1+I_2)}\mathrm{X}_1 + \frac{I_2}{(I_1+I_2)}\mathrm{X}_2 = \left(\frac{1}{1+T}\right)(\mathrm{X}_1 + T\cdot\mathrm{X}_2). \tag{5.17}$$

At this point I think an easier understanding by the reader is achieved giving a schematic illustration of the real setup this research group used, refer to figure 5.6.

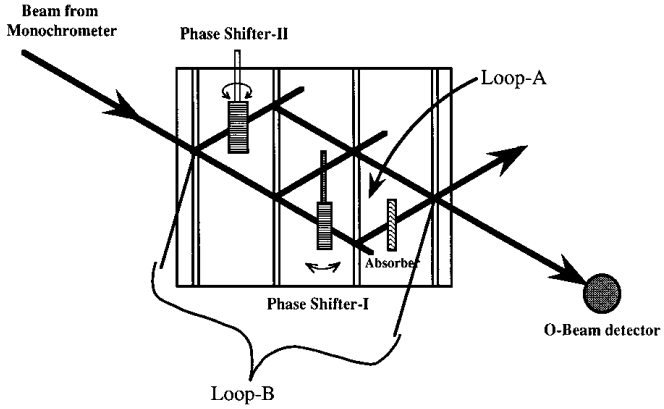

Figure 5.6 Experimental setup to observe the geometric phase by suppressing the dynamical phase using a dual-loop interferometer | ©Ref. 10

As one can understand from equation (5.17) the setup as shown in figure 5.6 can be designed in a way that the dynamical phase vanishes out. Thus, by choosing the right combination of the phase shifters and the absorber material the result is a measure of the geometrical phase alone. The cyclic evolution then means that the neutron quantum mechanical system evolves along the two paths of the interferometer and thereafter is caused to combine again. In this case, the Berry phase, depending on the curve C only, can be expressed in terms of the transmission probability T and the helicity σ, the latter term taking account of the combination of the neutron spin and its linear motion, to become

$$\phi_G(C) = 4\pi\sigma\frac{T}{1+T}. \tag{5.18}$$

The reason for having applied a two-loop interferometer in their experiment as illustrated in figure 5.6 can be easily understood from its advantageous feature, that is, the evaluation is carried out from unmistakable clicks provoked in the detectors at the end of the experimental course. Applying a normal one-loop interferometer would have given us classical intensities, and, from examining intensities only, the geometric phase would not have turned visible from our result, as I pointed out at the beginning of this section. That is the reason, why the group of Y. Hasegawa et al. used this special setup, where loop-A is used to generate the geometric phase, and where loop-B is a reference beam to determine the phase. Varying the combinations of the phase shifter I and an absorber in loop-A will generate various geometric phases i.e. loop-A performs the cyclic evolution of the wave function. They were also able to use the upper loss-beam in loop-A as a reference beam, because this beam interferes at the second crystal plate and thereby carries information of the second loop-B as well. An additional phase shifter II in loop-B gave the ability to observe and to measure the oscillation shifts due to Berry's phase.

Another experiment in this field was performed by A.G. Wagh, S.A Werner et al. [11], who implemented a sophisticated arrangement, which made that they did not even need to parallel transport the state, but which altogether yielded a non adiabatic, purely geometrical phase, and, moreover, which got rid of the dynamical phase in the end. Their experimental setup consisted of a three-crystal plate interferometer, in each path of it a dual spin flipper being inserted. In their turn, the Wagh et al. research group could verify the geometric phase as well.

Recently two papers were published ([14] and [15]), where the authors report about neutron experiments, in which they were able to balance the effect of the geometric phase by a change of Bell angles. To confirm the violation of a Bell like inequality they exposed one of the paths in an neutron interferometer to a radiofrequency field. They showed, that the value of S remained $2\sqrt{2}$ for all settings of the geometric phase.

5.4 Violation of Bell's inequality with a single neutron

We all remember very well when, around the beginning of quantum mechanics, John S. Bell eventually solved the big discussions between Albert Einstein and Niels Bohr by proposing us an inequality that has to be obeyed by any local hidden realistic theory. Many experiments in this area were made since, all emphasizing the same result, namely that in quantum mechanics a local hidden variable, which would make its theory realistic, does not exist, in other words, that local realism is untenable.

Also in the related field of conducting subtle Bell test experiments another goal could be achieved through neutron interferometer experiments. All experiments made until 2003 had been performed with two particles that got somehow entangled so that their correlations could be experimentally determined. Such complex procedure was no longer necessary when applying a neutron interferometer. In a paper by Y. Hasegawa and co. [13] an experimental setup was proposed that needed no more but a single neutron to successfully demonstrate the violation of a Bell-like inequality. A schematic picture of the setup they used for this experiment is shown in figure 5.7.

The principle they applied, simple though it may be, verifies to be efficient to an extraordinary extent. Their ingenious idea was not to entangle the same degrees of freedom associated with two different particles but to do so about two different degrees of freedom associated with one single neutron instead. They were able to do this because the observables of the spinor part of the neutron commuted with those of its spatial part. To describe the latter they defined α to be the part of the wave function influenced in spin and χ to be the part that undergoes a phase shift because of a spatial difference. So they obtained the whole wave function in terms of the first and the second degree of freedom to form a Bell state that satisfies

$$|\psi\rangle = \frac{1}{\sqrt{2}} \left(|\downarrow\rangle \otimes |I\rangle + |\uparrow\rangle \otimes |I\,I\rangle \right), \tag{5.19}$$

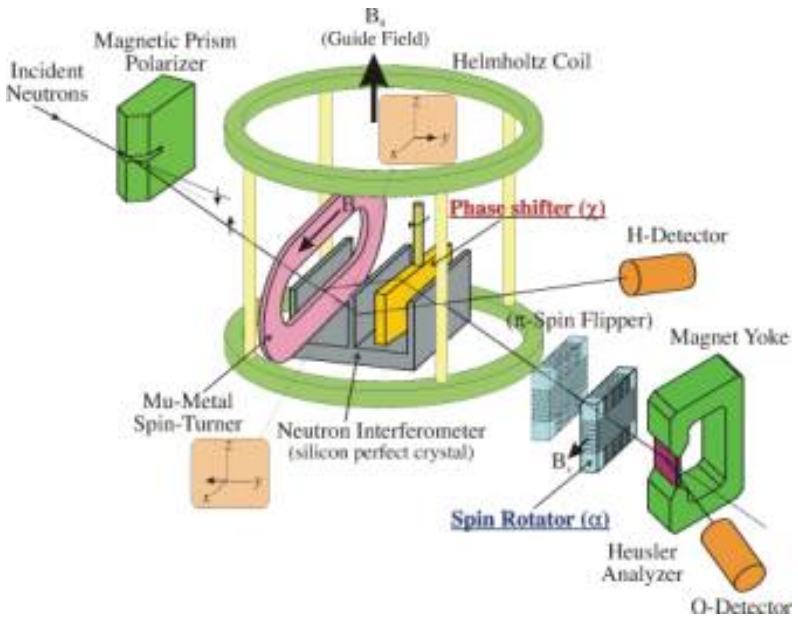

Figure 5.7 Experimental setup to violate Bell's inequality via a single neutron | ©Ref. 13

where the upwards arrow $\uparrow$ and the downwards arrow $\downarrow$ stand for the different spins, respectively, while I and II denote the two paths of the interferometer. The main part of the setup was the interferometer, which had been the *silicon-perfect-crystal interferometer beam line S18* at the Grenoble *Institut Laue-Langevin*. Further they used a phase shifter, realized by a slab of a certain material, as well as a spin-turner implemented via a sheet of Mu-metal, a high-permeable, 'soft' ferromagnetic alloy. The entering neutron beam splits at the first silicon crystal plate. Thereafter they had placed the spin turner, which in one path turns the spin of the neutron wavefunction into the direction that is opposite to that in the other path. Between the second and the third crystal plates they had put the path shifter, which causes an extra phase shift to the wave function when travelling along one path of the interferometer. They investigated the wave function upon its leaving the interferometer, analyzing the properties of the O-beam via spin-analysers and by a detector.

To carry out the evaluation they adopted a Bell-like inequality that allows to directly enter the counting rates for different spin angles α and phase shifts χ, then, using $N(\alpha, \chi)$ as the count rate for a certain spin rotation and for a certain phase shift, the experimental estimate for $E(\alpha, \chi)$ is calculated as

$$E(\alpha,\chi) = \frac{N(\alpha,\chi) + N(\alpha+\pi,\chi+\pi) - N(\alpha,\chi+\pi) - N(\alpha+\pi,\chi)}{N(\alpha,\chi) + N(\alpha+\pi,\chi+\pi) + N(\alpha,\chi+\pi) + N(\alpha+\pi,\chi)}. \tag{5.20}$$

After having completed the estimation of all $E(\alpha, \chi)$ values, which are subscripted with the corresponding integer indices, the experimental estimate of the test statistic S is found as

$$S = E(\alpha_1,\chi_1) + E(\alpha_1,\chi_2) - E(\alpha_2,\chi_1) + E(\alpha_2,\chi_2). \tag{5.21}$$

The authors report in their article that in one way or another the quality of the resolution of the obtained interference patterns was a problem, mainly due to losses at the second crystal plate, and to other experimental details. Nevertheless, they were able to tune their setup and could achieve visibility contrasts of more than 70%. In the end it was possible to show that the Bell-like inequality they used had been violated through a value of 2.051 ± 0.019, which is clearly greater than the magic limit of 2, that is, their experiment supports what quantum mechanics predicts. Their experimental settings had been $\alpha_1 = 0$ and $\alpha_2 = 0.5\pi$, respectively, as the 'Bell test angles', and 0.79π and 1.29π as the values for χ.

5.5 Outlook: Hypothetical deviation from the gravitational potential

A recent topic of the theoretical physics community arose from string theory, the only self-consistent quantum theory of gravity so far, and has initiated the seriously conducted discussion if the hypothetical deviations from the Newtonian gravitational potential [2] could exist, since these would allow us to better describe and understand for instance the postulated existence of dark energy. To assume the existence of such deviations led to postulating that gravitation spreads out in extra dimensions that are thought to be curled-up over tiny distances, the laws of gravity getting modified at distances comparable to the size of the extra dimensions and the number of the extra dimensions d_g determining the range of the spreading gravity, denoted as λ_s. For this deviating gravitational potential an extended approach has been set up in the following form

$$V(r) = -G\frac{mM}{r}\left(1 + \alpha e^{-\frac{r}{\lambda_s}}\right). \tag{5.22}$$

To check the feasibility of such investigations we apply the above formulation to evaluate for instance for the value of $d_g = 3$, what would give us a range λ_s of $10nm$. This fits the region of gravitational range where current experiments are getting performed, as for instance with the S18 beam line of thermal neutrons of the Laue-Langevin Institute. What exactly has our neutron interferometer to do with the postulation of extra dimensions in space? The link is held by the neutron-electron interaction that occurs upon the neutron scattering at the silicon crystal planes. Such a modified gravitational potential as formulated in (5.22) would lead us to a slightly different value of the scattering length of the neutrons when travelling across the affected silicon plate, our neutron interferometer yielding a very sensitive response to the modification. So we can say that with such thermal neutron interferometer and its related relatively simple experimental measurement it will well be possible to make investigations if our space has around additional 3 hidden extra dimensions. Together with the

physics community let us hopefully continue to watch the thrilling investigations launched into furnishing evidence of this triple 'hideaway'-brane.

6 Conclusion

"Anyone who is not shocked by quantum theory has not understood it." This is, what Niels Bohr once told us. When I started studying physics I had never learnt to understand Quantum Physics before, and then have got to consider it alarming to what extent the so-called *"philosopher in the street"* does not know from nothing. Still many more than one or another of the physicists remain satisfied by Quantum Physics, although to a varying degree, however, the ultimate questions that keep us excited about Quantum Mechanics will probably never loose their fascinating attraction. One of this exciting subjects is neutron interferometry as Helmut Rauch initiated it, providing us both a powerful and a very precise evaluation method to examine several quantum effects. In the field of Quantum Physics neutron interferometry has accomplished great success, and appears to continue doing so, in verifying many quantum phenomena in a very short period of time. Still, not all questions in Quantum Physics could be solved yet and therefore the applications of neutron interferometry keep covering a wide range for a next period of exciting investigations.

I wish to close quoting Richard P. Feynman, who gave the following statement on Quantum Mechanics: *"A philosopher once said, 'It is necessary for the very existence of science that the same conditions always produce the same results.' Well, they don't!"*

7 References

Text

[1] David Kendellen: “Neutron Interferometry and 4π Spinor Symmetry Experiments”; North Carolina State University, Raleigh, NC

[2] Michael Zawisky: Skriptum zur Vorlesung: “Neutronenoptik und Tomographie”; Atominstitut der √ñsterreichischen Universit√§ten

[3] Helmut Rauch: “Neutroneninterferometrie: Schl√ºssel zur Quantenmechanik”; Physik in unserer Zeit, 29. Jahrg. 1998, Nr.2

[4] Samuel A. Werner: “Neutron Interferometry”, Symposium in honour of Mike Rowe and Jack Rush, Sept 9, 2005, Gaithersburg, MD, (verhead transparencies)

[5] Samuel A. Werner: “Gravitational, Rotational and Topological Quantum Phase Shifts in Neutron Interferometry”; Class. Quantum Grav. 11 (1994), A207-A226

[6] R. Colella, A.W. Overhauser, S.A. Werner: “Observation of Gravitationally Induced Quantum Interference”; Phys. Rev. Lett. Vol. 34 Nr. 23, June 1975

[7] J. Anandan: “The Geometric Phase”; Nature Vol. 360, Nov. 1992

[8] J. Samuel, R. Bhendari; “General Setting for Berry’s Phase”; Phys. Rev. Lett. Vol. 60 Nr.23, June 1988

[9] K. Durstberger: “Berry Phase in an Entangled Spin-$\frac{1}{2}$ System”; Inst. for theoretical Physics, Univ. of Vienna

[10] Y. Hasegawa, M. Zawisky, H. Rauch: “Geometric Phase in Coupled Neutron Interference Loops”; Phys. Rev. A Vol. 53 Nr. 4, April 1996

[11] A.G. Wagh, V.C.Rakhecha, J. Summhammer, G. Badurek, H. Weinfurter, B.E. Allman, H. Kaiser, K. Hamacher, D.L. Jacobson, S.A. Werner: “Experimental Separation of Geometric and Dynamical Phases Using Neutron Interferometry”; Phys. Rev. Lett. Vol. 78 Nr. 5, February 1997

[12] A. Tomita, R.Y. Chiao: “Observation of Berry’s Topological Phase by use of an Optical Fiber”; Phys. Rev. Lett. Vol. 57 Nr. 8, August 1986

[13] Y. Hasegawa, R. Loidl, G. Badurek, M. Baron, H. Rauch: "Violation of a Bell-like Inequality in Single-Neutron Interferometry"; Nature Vol. 425, September 2003

[14] S. Sponar, J. Klepp, K. Durstberger-Rennhofer, R. Loidl, S. Filipp, M. Lettner, R.A. Bertlmann, G. Badurek, H. Rauch, Y. Hasegawa: "New Aspects of geometric Phases in Experiments with polarized Neutrons"; J. Phys. A: Math. Theor. Nr. 43, 2010, 15pp

[15] S. Sponar, J. Klepp, K. Durstberger-Rennhofer, R. Loidl, S. Filipp, M. Lettner, R.A. Bertlmann, G. Badurek, H. Rauch, Y. Hasegawa: "Geometric Phase in entagled Systems: A single-neutron Interferometer Experiment"; Phys. Rev. A, Nr. 81, 2010

Illustrations

- Figure 3.1: Wikipedia
- Figure 4.1: David Kendellen: "Neutron Interferometry and 4π Spinor Symmetry Experiments"(l); www.teilchen.at(r)
- Figure 4.2: Free Software Foundation
- Figure 4.3: M. Arif and D.L. Jacobson, NIST, 1997
- Figure 4.4: Michael Zawisky, Austrian Atomic Institute
- Figure 4.5: S.A. Werner
- Figure 4.6: Erwin Seidl
- Figure 5.1: David Kendellen: "Neutron Interferometry and 4π Spinor Symmetry Experiments"; North Carolina State University, Raleigh, NC
- Figure 5.2: Rauch et al., 1975
- Figure 5.3: R. Colella, A.W. Overhauser, S.A. Werner: "Observation of Gravitationally Induced Quantum Interference"; Phys. Rev. Lett. Vol. 34 Nr. 23, June 1975
- Figure 5.4: R. Colella, A.W. Overhauser, S.A. Werner: "Observation of Gravitationally Induced Quantum Interference"; Phys. Rev. Lett. Vol. 34 Nr. 23, June 1975

- Figure 5.5: J. Anandan; “The Geometric Phase”; Nature Vol. 360, Nov. 1992

- Figure 5.6: Y. Hasegawa, M. Zawisky, H. Rauch: “Geometric Phase in Coupled Neutron Interference Loops”; Phys. Rev. A Vol. 53 Nr. 4, April 1996

- Figure 5.7: Y. Hasegawa, R. Loidl, G. Badurek, M. Baron, H. Rauch: “Violation of a Bell-like Inequality in Single-Neutron Interferometry”; Nature Vol. 425, September 2003

8 Appendix

8.1 Curriculum vitae

Christian Gerald Knobloch

date of birth:	03.05.1989 in Melk
place of residence:	Aggsbach-Dorf 119, 3642 Aggsbach-Dorf
citizenship:	Austria
phone nr.:	0688/8226849
e-mail:	a0846069@univie.ac.at

Education

from 1995 to 1999:	*Elementary school* in Aggsbach-Dorf
from 1999 to 2003:	*Stiftsgymnasium* in Melk
from 2003 to 2007:	*High school at the Abby of Melk* focused on visual art
from 2007 to 2008:	*Zivildienst* at the red cross in Melk
since 2008:	Study of Physics at the University of Vienna

Personal skills and competences

- During the *Zivildienst* I was able to achieve the paramedic competence and I practice it since this time as a voluntary at the red cross.
- One of my favorite hobbies lays in the scientific exploration and documentation of caves.
- Because of this hobby I also joined the cave rescuers, where I can combine my knowledge of both special fields.
- In the summer of 2010 I worked for the *Veritas Verlag* as one of three coworkers to create a soluition-book for the math book of the sixth grade.